

Neurobiological Signatures of Anxiety and Depression in Resting-State Functional Magnetic Resonance Imaging

Desmond J. Oathes, Brian Patenaude, Alan F. Schatzberg, and Amit Etkin

ABSTRACT

BACKGROUND: There is increasing interest in using neurobiological measures to inform psychiatric nosology. It is unclear at the present time whether anxiety and depression are neurobiologically distinct or similar processes. It is also unknown if the best way to examine these disorders neurobiologically is by contrasting categorical definitions or by examining symptom dimensions.

METHODS: A cross-sectional neuroimaging study was conducted of patients with generalized anxiety disorder (GAD), major depressive disorder (MDD), comorbid GAD and MDD (GAD/MDD), or neither GAD nor MDD (control subjects). There were 90 participants, all medication-free (17 GAD, 12 MDD, 23 GAD/MDD, and 38 control subjects). Diagnosis/category and dimensions/symptoms were assessed to determine the best fit for neurobiological data. Symptoms included general distress, common to anxiety and depression, and anxiety-specific (anxious arousal) or depression-specific (anhedonia) symptoms. Low-frequency (.008–.1 Hz) signal amplitude and functional connectivity analyses of resting-state functional magnetic resonance imaging data focused on a priori cortical and subcortical regions of interest.

RESULTS: Support was found for effects of diagnosis above and beyond effects related to symptom levels as well as for effects of symptom levels above and beyond effects of diagnostic categories. The specific dimensional factors of general distress and anxious arousal as well as a diagnosis of MDD explained unique proportions of variance in signal amplitude or functional connectivity.

CONCLUSIONS: Using resting-state functional magnetic resonance imaging, our data show that a single conceptual model alone (i.e., categorical diagnoses or symptom dimensions) provides an incomplete mapping of psychopathology to neurobiology. Instead, the data support an additive model that best captures abnormal neural patterns in patients with anxiety and depression.

Keywords: Anhedonia, Anxiety, Depression, fMRI, Neuroimaging, Resting state

<http://dx.doi.org/10.1016/j.biopsych.2014.08.006>

A key issue for understanding the pathophysiology of mental illness as well as its nosology is the need to determine how symptoms relate to abnormal brain processes (i.e., putative mechanisms) (1). This issue is particularly salient for mood and anxiety disorders because comorbidity between disorders is the normative clinical course (2,3). One view that treats anxiety and depression as reflecting the same core process is supported by concordance studies indicating a shared genetic diathesis between generalized anxiety disorder (GAD) and major depressive disorder (MDD) (4,5). Symptom-based evidence also suggests a general class of “anxious-misery” disorders including GAD and MDD (6–8). However, these disorders can be differentiated with respect to illness predictors and symptoms (3,9–11). Comparisons between GAD and MDD indicate greater emotion intensity and goal motivation in GAD and lower positive affect in MDD, among other factors (10).

Not only is it unclear to what degree GAD and MDD are similar or different as disorders, but also it is unclear whether

categorical definitions of GAD and MDD best capture abnormalities. Many authors have argued for understanding anxiety and depression as a set of distinct and overlapping dimensions of dysfunction (12,13). One of the most well-known models (13–15) proposes a tripartite organization: a shared general factor (general negative affect or distress) and two specific factors—*anxious arousal* (more central to anxiety) and *low positive affect or anhedonia* (more central to depression).

Complicating a clearer understanding of the neurobiology of anxiety and depressive disorders is the fact that few studies directly compare patients across these diagnostic groups (16–18). In a more recent study, we found that only patients with GAD (with or without MDD) showed a behavioral deficit in emotion regulation; this was not present for patients with MDD only (19). This deficit reflected an abnormality in cingulate-amygdala circuitry normally required for this task (20) as well as a unique (compensatory) pattern of activation in patients with MDD only. In a study of anxious and depressed adolescents, Beesdo *et al.* (21) found both common and disorder-specific

abnormalities in amygdala activation during emotional face processing. All patients had greater amygdala activation to fear faces when focused on their own emotions, but facial affect interactions divided patients into complex patterns during passive viewing.

Broadly comparing anxiety and depression, it may be advantageous to examine task-independent brain activity, allowing assessment across brain regions that may not be involved in a particular task. A powerful tool for doing so is resting-state functional magnetic resonance imaging (fMRI), in which intrinsic activity and connectivity of brain circuitry can be examined across many brain systems and regions (22). Separate resting-state studies of patients with GAD and patients with MDD have implicated abnormalities in many structures, including amygdala, hippocampus, ventral striatum, insula, dorsal and subgenual anterior cingulate (ACC), and dorsolateral and medial prefrontal cortices (DLPFC, mPFC) (23–32). It is still unclear how these brain areas covary in patients as a function of pathophysiology. Analyses of the relationship between anxiety symptoms in healthy subjects and resting-state brain activity have demonstrated effects in many of these same regions (33–35). However, to our knowledge, anxiety and depression have never been directly compared using task-independent resting-state methods, and categorical and dimensional conceptualizations have not been evaluated in a single cohort.

In this study, we sought to answer the following three questions: 1) Are neural signatures of anxiety and depression consistent with their being common or distinct neurobiological processes? 2) What are the relative contributions of categorical and dimensional formulations of anxiety and depression on neural processes? 3) Which brain regions are most strongly related to anxiety and depression? We analyzed models of combined categorical and dimensional factors according to the amplitude of the low-frequency resting-state signal within each region as well as functional connectivity between regions, measured as time series correlations between region pairs. All participants were medication-free when scanned.

To ensure a comprehensive categorical analysis, we recruited participants with a diagnosis of GAD, with a diagnosis of MDD, with both diagnoses, or with neither diagnosis. Because these three groups overlapped by symptom profiles, we were similarly able to conduct dimensional analyses. For the categorical analyses, separate predictors corresponding to a diagnosis of GAD or MDD allowed us to examine disorder-specific effects, whereas a single predictor corresponding to either diagnosis tested for a general patient deficit relative to controls. By having partially overlapping patient groups and modeling diagnoses together, we allowed for the possibility that abnormalities in one diagnostic group (e.g., MDD) could be best explained by its frequent comorbid diagnosis (e.g., GAD) or the possibility that individual diagnoses could explain independent neural abnormalities even after accounting for the presence of the other diagnosis. For dimensional analyses, we used the Mood and Anxiety Symptom Questionnaire (36), developed to assess the common symptom domain of general distress elevated across anxiety and depressive disorders, and specific domains of anxious arousal and anhedonia in accordance with the dimensional tripartite model of anxiety and depression. Three separate models were run for each metric (signal amplitude and functional connectivity): individual

categorical and dimensional models were first run to establish possible relationships between these factors and brain measures. Next, to understand further the primacy of either categorical or dimensional measures for explaining variability in brain measures, we combined categorical and dimensional measures in a simultaneous regression. This strategy allowed for uncovering additive or overlapping predictors across categories and dimensions depending on which measures were the strongest predictors and which explained unique brain variability after accounting for the other factors.

METHODS AND MATERIALS

Participants

After providing informed consent, 90 subjects participated in this study; these subjects largely overlapped with the subjects reported in our articles on task-based fMRI (19,23,37). Current-episode DSM-IV-based psychiatric diagnoses (38) were determined with the Mini International Neuropsychiatric Interview (39,40). Participants included 38 healthy control subjects, 17 subjects with a primary diagnosis of GAD and no MDD, 12 subjects with a primary diagnosis of MDD and no GAD, and 23 subjects with both diagnoses (see Table S1 in Supplement 1 for other comorbidities). Exclusion criteria were the presence of substance abuse or posttraumatic stress disorder; a history of a neurologic disorder or severe mental illness (psychosis or bipolar); a history of head trauma or loss of consciousness; claustrophobia; or regular use of benzodiazepines, opiates, or thyroid medications. All control subjects were free of current or past Axis I conditions or psychiatric medications. No patient took a benzodiazepine within 48 hours of the scan, and all patients were free of antidepressant medication for >6 weeks.

fMRI Data Acquisition and Processing

Neuroimaging data were acquired on a 3-Tesla GE Signa scanner (GE Healthcare, Milwaukee, Wisconsin) using a custom-built eight-channel head coil. Functional data were acquired in 29 axial slices (4.0-mm thickness, .5-mm gap) across the whole brain using a T2*-weighted gradient echo spiral (in/out) sequence (repetition time = 2 sec; echo time = 30 msec; flip angle = 80°; 1 interleaf; field of view = 22 cm; 64 × 64 matrix; 236 volumes) (41). Instructions for the 8-min resting-state scan asked participants to keep still, keep their eyes closed, and let their mind wander. An automated high-order shim for spiral acquisitions was used before acquiring fMRI data (42). A high-resolution T1-weighted three-dimensional inversion recovery spoiled gradient recoil anatomic scan (inversion time = 300 msec; repetition time = 8 msec; echo time = 3.6 msec; flip angle = 15°; field of view = 22 cm; 124 coronal plane slices; matrix = 256 × 192; 2 excitations; acquired resolution = 1.5 mm × 0.9 mm × 1.1 mm) was acquired in the same session as fMRI data.

Physiologic variability recorded in respiration and heart rate pulse oximetry was used for fMRI data correction as an initial preprocessing step (image based using acquisition timing relative to phases of cardiac and respiratory cycles) (43). Motion (middle volume reference; 12 degrees of freedom affine, FSL FLIRT [FMRIB Linear Image Registration Tool, University of

Oxford, Oxford, United Kingdom] defaults) and then slice timing correction was applied to functional images; no participant had movement >3 mm translation or 3 degrees of rotation (cumulative, absolute value). Affine registration of the functional to structural images was combined with nonlinear normalization between T1 and MNI152 space for functional images using standard settings for the FSL 5.0 FNIRT tool (<http://fsl.fmrib.ox.ac.uk/fsl/fslwiki/>). Functional images were smoothed with a 5-mm full width at half maximum Gaussian filter. Time series data were band-pass filtered (.008–.1 Hz) and entered in a first-level fixed-effects general linear model for functional connectivity calculation, covarying for white matter and cerebrospinal fluid signal (see Supplement 1 for analyses of this noise estimate) as well as residual motion parameters. Fisher's r -to- z calculation on functional connectivity images was performed before average connectivity values were extracted across each region of interest (ROI). The Data Processing Assistant for Resting-State fMRI (<http://rfmri.org/DPARSF>) toolbox (44) was used on unfiltered data to generate spectral power amplitudes in the low-frequency band (.008–.1 Hz). The root mean square of the power spectrum density in the chosen band was standardized to the average amplitude of the full gray matter mask (voxel/average rest of brain). Then fractional amplitude was calculated relative to the full power spectrum (low frequency/full band) defined by the fMRI sampling rate (0–.25 Hz for repetition time = 2.0) and was used for ROI extraction and analysis, referred to hereafter as “signal amplitude.”

ROI Selection

A priori ROI were defined (Figure 1) where possible by anatomic boundaries, including the hippocampus (70% probability threshold in the Harvard-Oxford atlas) (45), basolateral and centromedial amygdala (maximum probability defined in our previous article, from a cytoarchitecturally defined atlas) (23,46), and the ventral striatum (based on subcortical anatomic segmentation atlas (47) with a small overlap in the left hemisphere with the subgenual ACC ROI removed). Amygdala extractions used a combined basolateral and centromedial mask because separating the amygdala by subregion did not alter findings. The subgenual ACC ROI was an 8-mm gray matter-masked sphere around a peak coordinate (x, y, z : 2, 18, -8) associated with MDD abnormalities averaged from 14 fMRI studies (48). The ROI for the dorsal ACC, DLPFC, mPFC, and fronto-insular cortex were derived by thresholding resting-state independent component maps from a separate cohort of healthy subjects to yield 1000 voxel clusters for each region to allow them approximately equal weight as seeds for cross-region comparisons, in accordance with the topography of typical resting-state networks (49). For nonmidline regions, we averaged signal from left-sided and right-sided ROI, given no laterality predictions and an exploratory principal component analysis indicating left and right hemisphere signal amplitude and connectivity loading consistently on the same factor.

Statistical Analyses

Mean low-frequency signal amplitudes and functional connectivity (Z score) values for each ROI were determined in Montreal Neurological Institute space. Using SPSS software (SPSS, Inc., Chicago, Illinois), we conducted principal

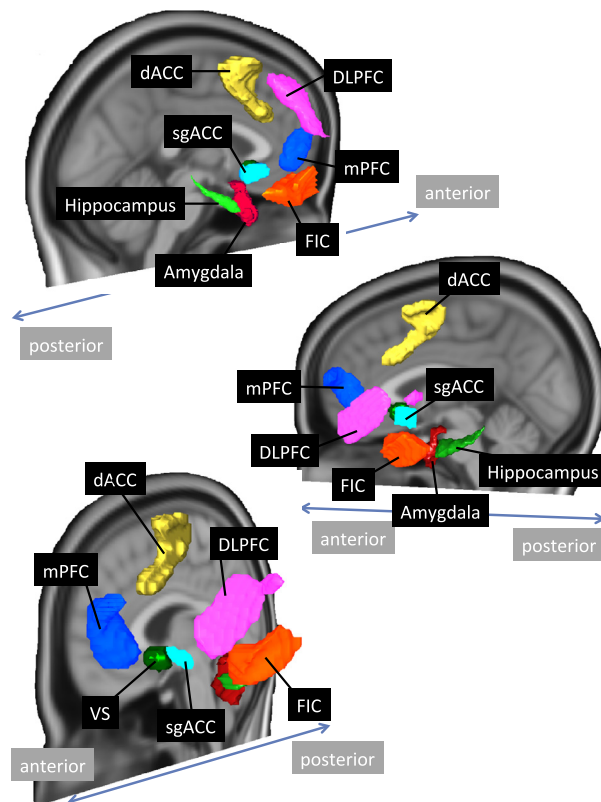


Figure 1. Brain image depicts surface reconstructions of regions of interest used in functional connectivity and intrinsic signal amplitude analyses. dACC, dorsal anterior cingulate cortex; DLPFC, dorsolateral prefrontal cortex; FIC, fronto-insular cortex; mPFC, medial prefrontal cortex; sgACC, subgenual anterior cingulate cortex; VS, ventral striatum.

components analyses with quartimax rotation for data reduction to limit multiple comparisons and to recognize that dimensional and categorical constructs related to affective disorders probably involve several distributed neural processes. For specific component interactions with categorical or dimensional variables, stepwise regressions were included to determine standardized β ($s\beta$) and significance values for individual predictors (stepping criteria, entry, .05; removal, .10). The optimal number of extracted components was determined by eigenvalues >1 . Identical analyses were run separately for signal amplitude and functional connectivity Z scores. Resting-state data were analyzed using general linear models, including principal components as repeated measures with a Greenhouse-Geisser correction, as described in the Results. χ^2 and t tests were used where noted.

RESULTS

Sample Characteristics

No significant differences in age, education, gender, or average head motion (x, y, z directions) were found using either categorical or dimensional models (all $p > .08$) (Table S1 in Supplement 1). As shown in Figure 2, there was partial overlap in symptom scores between control subjects and

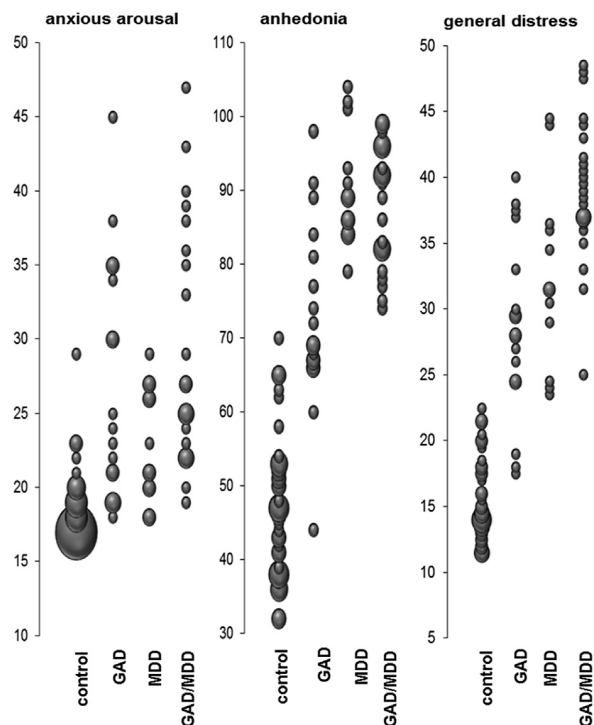


Figure 2. Distribution of the dimensional Mood and Anxiety Symptom Questionnaire subscale scores across each of the diagnostic categories. Sphere size represents the frequency of responses. GAD, generalized anxiety disorder; MDD, major depressive disorder.

patients, motivating our primary analytic approach of including data from all participants, supplemented by a follow-up analysis restricted to patients (Supplement 1).

Low-Frequency Signal Amplitudes

To minimize the number of comparisons, our principal components data reduction across ROI yielded three principal components. As shown by rotated component loadings in Table 1, these involve primarily limbic/paralimbic regions (amygdala, hippocampus, ventral striatum, subgenual ACC), DLPFC/mPFC, and cingulo-opercular regions (dorsal cingulate and fronto-insular cortex). We entered these three components as repeated measures into three general linear models examining 1) categorical predictors only (GAD, MDD), 2) dimensional predictors only (anxious arousal, anhedonia, general distress), and 3) categorical and dimensional predictors together to determine the strongest independent predictors of signal amplitude.

For categorical predictors only, we found a GAD by principal component interaction [$F_{2,172} = 1.4, p = .036$] and a marginal GAD by MDD interaction [$F_{1,86} = 2.8, p = .096$; other $p > .12$]. As shown in Figure 3A, the GAD by principal component interaction reflected a GAD effect specifically on limbic/paralimbic regions, wherein greater low-frequency signal amplitudes were seen for participants with GAD compared with participants without GAD [$t_{88} = 2.5, p = .015$; other $p > .28$]. In a stepwise model, only GAD was a significant predictor of limbic/paralimbic signal ($\beta = .255, p = .015$).

We also examined in a repeated measures model whether patients as a whole differed from control subjects in low-frequency signal amplitudes, but we found no main effect of patient versus control subject or interaction with principal component (all $p > .40$).

For dimensional predictors only, we found interactions of principal component with both anhedonia [$F_{2,172} = 3.5, p = .034$] and general distress [$F_{2,172} = 5.3, p = .006$]. The interaction with anhedonia was driven by correlations that differed slightly by component (slightly positive, slightly negative, and nil) but without approaching significance (all $p > .21$). General distress was specifically positively related to limbic/paralimbic low-frequency signal amplitudes in the stepwise model ($\beta = .248, p = .019$; other factors $p > .13$) (Figure 3B), driving the full model interaction.

Despite the fact that symptom scores were continuously distributed and partially overlapping between patients and control subjects, effects of dimensional predictors across participants may still reflect higher symptom scores in patients. We tested a model that included the three dimensional predictors, a categorical predictor for patient versus control subject, and the interactions between the categorical patient predictor and dimensional symptom predictors. Nonetheless, we still found the significant interaction between principal component and general distress [$F_{2,170} = 6.33, p = .002$], no significant interaction with anhedonia [$F_{2,170} = 1.11, p = .331$], and no interactions or main effects for the patient predictor (all $p > .29$).

Finally, we tested the combination of categorical and dimensional predictors to determine which predictors account for the greatest variance in low-frequency signal. Because both GAD and general distress were associated with greater limbic/paralimbic signal in the separate categorical and dimensional models, respectively, we were particularly interested in which was the stronger predictor in a combined model. We found that the principal component by general distress interaction remained significant [$F_{2,168} = 5.0, p = .008$], again driven by a positive relationship with limbic/paralimbic signal (Figure 3C), whereas the GAD main effect was reduced to nonsignificance [$F_{1,84} = .1, p = .824$] indicating that distress substantially overlapped with the GAD effect and was an even better predictor of limbic/paralimbic low-frequency signal amplitude (forced entry GAD first block, $\beta = .255, p = .015$; second block stepwise remaining variables, $p > .29$). There was a marginal component by MDD interaction [$F_{2,168} = 2.76, p = .066$] and a significant MDD main effect [$F_{1,84} = 5.62, p = .020$] driven by lower signal amplitudes for MDD (Figure 3D; Figure S1 in Supplement 1). After accounting for relationships between signal amplitude and all other factors from each of the three symptom scales and GAD diagnosis (estimated marginal means), MDD was the only factor associated with reduced signal amplitudes. Parallel analyses on the 52 patients only revealed highly similar findings (Supplement 1), demonstrating consistency and robustness of findings.

Functional Connectivity

Principal component data reduction on all ROI pairwise functional connectivity correlations yielded six components (Table 1). The first component captured cortical connectivity (nonsubcortical); the second, subgenual cingulate and ventral

Table 1. Data Reduction for Low-Frequency Signal Amplitude and Functional Connectivity Data^a

Signal Amplitude Principal Components						
Region	Limbic/Paralimbic		DLPFC/MPFC		Cingulo-Opercr	
sgACC	.848 ^b		.236		.082	
VS	.826 ^b		.278		.059	
Amyg	.702 ^b		-.211		-.217	
Hippo	.376 ^b		-.145		.028	
mPFC	.146		.868 ^b		.092	
DLPFC	-.135		.840 ^b		-.110	
dACC	-.245		.175		.791 ^b	
FIC	.309		-.253		.749 ^b	
Functional Connectivity Principal Components						
Connectivity Pair ^c	Cortical	sgACC/VS	Amyg-Sub	Amyg-Pfc	Fronto-Operc	Amyg-Fronto-Operc
Hippo ↔ dACC	.880 ^b	-.025	.041	.033	-.114	.226
Hippo ↔ FIC	.852 ^b	.017	.027	-.198	.023	.344
Hippo ↔ DLPFC	.827 ^b	.035	-.026	.275	-.080	-.014
VS ↔ dACC	.802 ^b	.061	.118	-.205	-.190	-.174
mPFC ↔ dACC	.798 ^b	-.008	.011	-.107	.465 ^b	.038
sgACC ↔ dACC	.798 ^b	.098	.059	-.373	-.109	-.184
VS ↔ DLPFC	.794 ^b	.184	.020	.088	-.078	-.395
FIC ↔ mPFC	.793 ^b	.134	-.143	-.135	.398	.127
mPFC ↔ DLPFC	.768 ^b	-.210	.053	.022	.285	-.226
VS ↔ FIC	.755 ^b	.218	-.005	-.436	-.164	.082
FIC ↔ DLPFC	.755 ^b	.083	-.097	.146	.489 ^b	-.112
sgACC ↔ FIC	.739 ^b	.249	-.051	-.510 ^b	-.073	.102
Amyg ↔ DLPFC	.736 ^b	-.051	.178	.434 ^b	.039	.224
sgACC ↔ DLPFC	.733 ^b	.088	.004	-.146	-.120	-.475 ^b
FIC ↔ dACC	.728 ^b	.010	.067	.096	.126	-.111
Amyg ↔ dACC	.716 ^b	-.065	.179	.223	-.232	.441 ^b
Hippo ↔ mPFC	.685 ^b	.379	-.053	.391	-.169	-.008
Amyg ↔ FIC	.676 ^b	-.163	.396	-.086	-.096	.448 ^b
DLPFC ↔ dACC	.656 ^b	-.026	-.026	.092	.625 ^b	.032
Amyg ↔ mPFC	.643 ^b	.154	.413	.472 ^b	.031	.128
sgACC ↔ VS	.295	.797 ^b	.075	-.105	.181	.071
Hippo ↔ sgACC	.390	.686 ^b	.207	-.043	.092	.009
Hippo ↔ VS	.497	.655 ^b	.108	.034	-.192	.036
VS ↔ mPFC	.557 ^b	.608 ^b	-.054	.219	-.063	-.153
sgACC ↔ mPFC	.444	.580 ^b	.042	-.031	-.253	-.354
Amyg ↔ VS	.464	.247	.742 ^b	.025	-.060	.014
Amyg ↔ sgACC	.350	.371	.718 ^b	-.106	.176	-.025
Amyg ↔ Hippo	.371	-.053	.703 ^b	.102	-.111	.022

ACC, anterior cingulate cortex; Amyg, amygdala; dACC, dorsal anterior cingulate cortex; DLPFC, dorsolateral prefrontal cortex; FIC, fronto-insular cortex; Hippo, hippocampus; mPFC, medial prefrontal cortex; Operc, operculum; Pfc, prefrontal cortex; sgACC, subgenual anterior cingulate cortex; VS, ventral striatum.

^aColumn heads refer to brain areas or connectivity pairs with higher loadings that especially contribute to individual factors.

^bRegions or pairs with higher loadings.

^cThe symbol ↔ indicates functional connectivity between brain regions listed to the left and right of the symbol.

striatum connectivity; the third, amygdala subcortical connectivity; the fourth, positive amygdala prefrontal (and negative fronto-opercular subcortical) connectivity; the fifth, prefrontal fronto-opercular connectivity; and the sixth, amygdala to fronto-opercular connectivity. Entering these into a repeated measures model with only categorical predictors did not produce any significant findings (all $p > .23$). With the dimensional only model, there was a component main effect

[$F_{5,430} = 2.5, p = .029$] and a factor by anxious arousal interaction [$F_{5,430} = 2.6, p = .027$; other $p > .20$]. In the follow-up stepwise regressions, the only significant model was for subgenual ACC/ventral striatum connectivity [$F_{1,89} = 7.33, p = .008$] driven by a positive relationship with anxious arousal ($\beta = .277, p = .008$; excluded variable $p > .81$) (Figure 4A). We were especially interested in whether this relationship held when controlling for diagnoses in the same model.

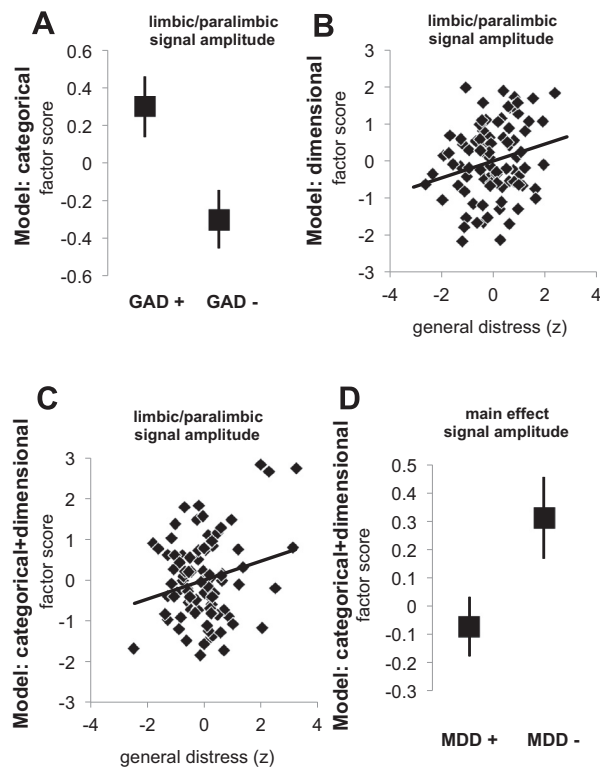


Figure 3. Signal amplitude results from categorical models, dimensional models, or both categorical and dimensional models of anxiety and depression for all participants, plotting estimated marginal means and standard errors. **(A)** For the categorical model, a specific effect of generalized anxiety disorder on limbic/paralimbic signal amplitude was found. **(B)** For the dimensional model, there was a significant positive relationship between the broad symptom of general distress and limbic/paralimbic signal amplitude that remained significant in the combined categorical and dimensional model **(C)** after accounting for other symptoms and diagnostic categories. **(D)** In the combined model, a main effect of major depressive disorder was driven by overall lower signal amplitudes for patients with depression compared with individuals without depression. GAD, generalized anxiety disorder; MDD, major depressive disorder.

In the model with both categorical and dimensional predictors, the component by anxious arousal interaction was marginally significant [$F_{5,420} = 2.1, p = .065$]. The positive relationship between anxious arousal and subgenual ACC/ventral striatum connectivity remained significant (Figure 4B), whereas the other variables did not contribute additional explanatory power (forced entry anxious arousal first block, $s\beta = .277, p = .008$; second block stepwise remaining variables, all $p > .35$). There was also a marginal component by anhedonia interaction [$F_{5,420} = 2.0, p = .077$] and a significant interaction between component and MDD diagnosis [$F_{5,420} = 2.5, p = .029$]. To follow up the MDD interaction, regressions for each component testing marginal means covarying the other factors suggested that the effect was driven by lower subgenual ACC/ventral striatum connectivity [$F_{1,84} = 5.4, p = .022$] (Figure 4C) and greater amygdala subcortical connectivity [$F_{1,84} = 4.2, p = .043$] (Figure 4D) for patients with MDD (other $p > .24$). An overlap in findings across the models suggests that anxious arousal drives up

subgenual ACC/ventral striatum connectivity independent of the influence of MDD diagnosis that drives down connectivity in the same circuit. Findings in patients indicated the same patterns (Supplement 1).

DISCUSSION

To our knowledge, this is the first study to compare directly anxiety and depressive disorders with resting-state fMRI and to explore explicitly both categorical and dimensional conceptualizations of these conditions together relative to one another. Our findings lend support for both commonalities and distinctions between anxiety and depression. These findings suggest that neither a categorical nor a dimensional model of anxiety and depression explains neurobiology to the exclusion of the other. Rather, mapping the affective pathology onto neurobiological substrates requires combining categorical and dimensional specifications of anxiety and depressive disorders. The combination accounted for patterns of overlapping and independent predictors of resting-state fMRI brain measures. More specifically, our data argue that general distress increases limbic/paralimbic low-frequency signal amplitudes, whereas MDD diagnosis drives signal down across the brain areas we studied. In terms of functional connectivity between ROI, anxious arousal was associated with greater subgenual ACC/ventral striatum connectivity, whereas MDD was associated with reduced connectivity in this same circuit when covarying symptoms and GAD diagnosis. The anxiety and distress correlations remained significant with or without covarying symptoms and diagnoses. Both relationships were also significant in the patient group alone indicating relevance to affective pathology. The regions most important for understanding both categorical and dimensional aspects of anxiety and depression were the amygdala, ventral striatum, hippocampus, and subgenual ACC. These regions are consistently implicated in anxiety-relevant and depression-relevant processes, such as threat processing, reward and motivation, affect regulation, and memory.

With regard to whether anxiety and depression are components of a single psychopathologic process or reflect distinct processes, we found that categorical diagnoses MDD and GAD are associated with distinct resting-state alterations. However, the GAD effect (greater limbic/paralimbic signal) is better attributed to the symptom dimension of general distress. General distress can be considered a measure of disorder-nonspecific broad negative affect, and similar results (not shown) are found by replacing this measure with the first principal component from a principal component analysis across many depression and anxiety measures [Beck Anxiety and Depression Inventories (50,51), Penn State Worry Questionnaire (52), Spielberger Trait Anxiety Inventory (53)]. However, the categorical effect of MDD was especially strong in patients and represented a nonoverlapping suppression of signal amplitude across ROI. In functional connectivity, anxious arousal emerged as a strong independent predictor of increased subgenual ACC/ventral striatum connectivity in the opposite direction of an MDD effect (covarying GAD diagnosis and other symptoms). We found diagnosis-specific perturbations related to MDD as well as diagnosis-nonspecific perturbations related

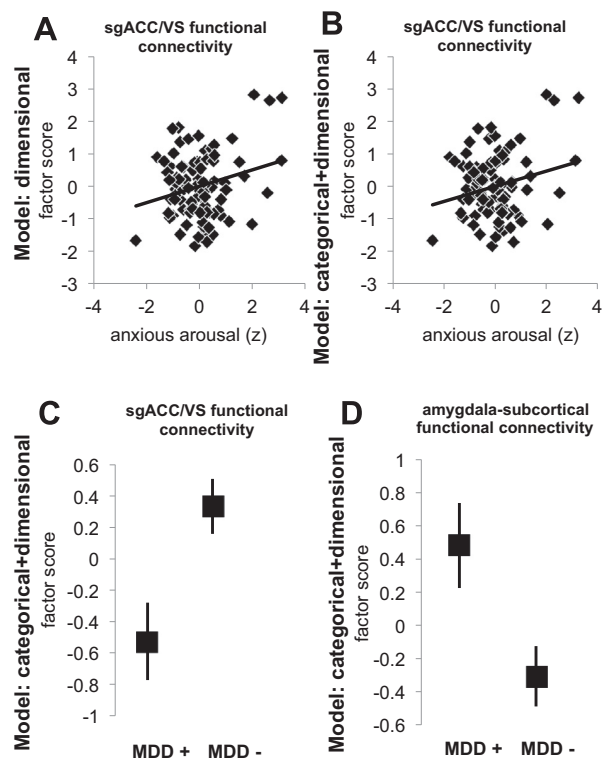


Figure 4. Functional connectivity results from categorical models, dimensional models, or both categorical and dimensional models of anxiety and depression for all participants, plotting estimated marginal means and their standard errors. **(A)** For the dimensional model, there was a significant relationship between anxious arousal and connectivity with the subgenual anterior cingulate cortex/ventral striatum that was again significant in the combined categorical and dimensional model **(B)**. In the combined model, major depressive disorder was associated with reduced subgenual anterior cingulate cortex/ventral striatum connectivity **(C)** and increased amygdala-subcortical connectivity **(D)**. MDD, major depressive disorder; sgACC, subgenual anterior cingulate cortex; VS, ventral striatum.

to general distress and anxious arousal. Although there were small differences between models, results were strikingly consistent at multiple levels (full group and patients alone) and with or without covarying other categorical/dimensional factors.

Our findings have implications not only for how neurobiology can inform psychopathology and its nosology but also for emerging theoretical models of mental illness. A DSM-type approach relies on specific symptom criteria for establishing a categorical diagnosis, whereas an approach such as the Research Domain Criteria from the National Institute of Mental Health advocates for a dimensional organization. Our data suggest that use of only a single conceptual framework (i.e., categorical diagnoses or symptom dimensions) provides an incomplete answer. Although it may, in principle, be possible to establish dimensions that capture the MDD diagnosis effect, it is apparent that one of the best-described attempts to do so (i.e., the tripartite model) was insufficient for this application. As a predictor for our brain measures, GAD was subsumed under general distress. Also, MDD emerged primarily as an effect only when accounting for GAD and

dimensional scales (combined model). One possibility is that symptoms are especially strong predictors of resting brain abnormalities but could partially obscure a weaker but distinct MDD categorical abnormality. The functional relevance of both dimensional and categorical predictors should be carried forward as an investigation for future research. The patient only correlation between distress and DLPFC/mPFC connectivity did not reflect an abnormality in models with healthy controls but nevertheless may reflect important within-patient clinical phenomena given especially the importance of these regions for mapping individual differences in MDD response to transcranial magnetic stimulation (48,54).

Methodologically, it is notable that our findings suggest unique sources of pathology across domains of low-frequency signal amplitude and low-frequency correlation (functional connectivity) between brain regions implicated in clinical anxiety and depression. Nevertheless, theoretical overlaps can be seen across the two measures. For example, anxious arousal was associated with greater subgenual ACC/ventral striatum connectivity, and general distress was associated with greater signal for a factor that included these brain areas (limbic/paralimbic factor). Also, an MDD diagnosis was associated broadly with lower signal amplitudes consistent with lower subgenual ACC/ventral striatum connectivity findings for MDD. However, anxious arousal was also associated with lower amygdala connectivity to a specific target (fronto-opercular), and MDD was associated with greater amygdala-to-subcortical connectivity, which represent a seemingly unrelated set of abnormalities. Low-frequency signal amplitude is a reliable fMRI blood oxygen level-dependent derivative (55) sensitive to both stable individual differences (56) and transient brain fluctuations (49). However, it is used far less frequently than independent component analysis or functional connectivity to study resting brain networks, and the degree of complementarity between signal amplitude and these traditional measures warrants added attention including in the domain of psychopathology.

Limitations of this study include a relatively small sample of patients with MDD alone (see also power calculations in Supplement 1 regarding MDD only effects). Nonetheless, sample sizes were substantial across disorders for comparing effects for anxiety and depression as general groupings. Also, our groups were well educated, on average, which may have influenced findings. Allowing some comorbidity increased the representativeness of our sample but may also have influenced results. A limitation of resting-state fMRI is that the nature of the measures in isolation precludes insight about specific mental processes. Future work will need to extend these findings using tasks more directly tapping functions subserved by key regions identified here and with appropriate manipulations and assessments of mental states related to psychopathology at rest. Resting-state networks are largely stable across behavioral states, levels of consciousness, and species (57), which suggests that resting-state measures may capture consistent mental state differences between patients and healthy individuals. Our data likely speak to broad baseline neuropathology that may be superimposed on or interact with brain signatures of specific mental states (that also may differ by patient group). Additional descriptions of patients using other factors (e.g., cognitive symptoms, perseverative thinking, functional impairment) may explain additional variance compared with these

initial models. Similarly, additional brain regions or networks could contribute further evidence of patient abnormalities related to dimensions and categories. Methodologically, increasing the number of transmit/receive coils could improve signal-to-noise ratio and lead to additional findings (perhaps better resolution of amygdala subregional effects). Typical psychiatric medications influence the neural circuitry studied here, and because many patients regularly take these medications, a follow-up study might include patients taking medication to understand how the metrics observed in the present study are influenced by specific medications.

In conclusion, our results provide support for a combination of categorical and dimensional conceptualizations of anxiety and depression and illustrate both the condition-specific perturbations and the perturbations related more broadly to affective distress. Use of a broadly applicable neurobiological measure, resting-state fMRI, has provided a powerful brain-based test of dominant conceptual models of anxiety and depression developed through the study of symptoms and diagnostic categories.

ACKNOWLEDGMENTS AND DISCLOSURES

This work was supported by the War Related Illness and Injury Study Center Special Fellowship Program at Veterans Affairs Palo Alto and the Medical Research Service of the Department of Veterans Affairs, Veterans Affairs Palo Alto (DJO); National Institute of Mental Health Grant Nos. P30MH089888 (AFS) and R01MH091860 (AE); and Sierra-Pacific Mental Illness Research Education and Clinical Center at Veterans Affairs Palo Alto Health Care System.

AFS has served as a consultant to BrainCells, CeNeRx, BioPharma, CNS Response, Corcept Therapeutics, Eli Lilly and Company, Forest Laboratories, GlaxoSmithKline, InnoPharma, Lundbeck, Merck & Co., NeuroNetics, Novartis, Pathway Diagnostics, Pfizer, PharmaNeuroBoost, Quintiles, Sanofi, Synosis, Takeda and Xytis; has equity in Amnestix, BrainCells, CeNeRx, Corcept Therapeutics (cofounder), Forest Laboratories, Merck, Neurocrine Biosciences, Pfizer, PharmaNeuroBoost, Somaxon Pharmaceuticals, and Synosis; was named an inventor on pharmacogenetic use patents on prediction of antidepressant response; and has received speaking fees from GlaxoSmithKline and Roche. The other authors report no biomedical financial interests or potential conflicts of interest.

ARTICLE INFORMATION

From the Department of Psychiatry and Behavioral Sciences (DJO, BP, AFS, AE), Stanford University, Stanford, and Sierra-Pacific Mental Illness Research, Education; and Clinical Center (DJO, BP, AE), Veterans Affairs Palo Alto Health Care System, Palo Alto, California, USA.

Address correspondence to Amit Etkin, M.D., Ph.D., Department of Psychiatry and Behavioral Sciences, Stanford University, 401 Quarry Road, MC: 5797, Stanford, CA 94305-5797; E-mail: amitetkin@stanford.edu.

Received Dec 19, 2013; revised Aug 5, 2014; accepted Aug 6, 2014.

Supplementary material cited in this article is available online at <http://dx.doi.org/10.1016/j.biopsych.2014.08.006>.

REFERENCES

- Insel T, Cuthbert B, Garvey M, Heinssen R, Pine DS, Quinn K, *et al.* (2010): Research domain criteria (RDoC): Toward a new classification framework for research on mental disorders. *Am J Psychiatry* 167: 748–751.
- Brown TA, Campbell LA, Lehman CL, Grisham JR, Mancill RB (2001): Current and lifetime comorbidity of the DSM-IV anxiety and mood disorders in a large clinical sample. *J Abnorm Psychol* 110: 585–599.
- Kessler RC, Gruber M, Hetttema JM, Hwang I, Sampson N, Yonkers KA (2008): Co-morbid major depression and generalized anxiety disorders in the National Comorbidity Survey follow-up. *Psychol Med* 38:365–374.
- Kendler KS, Neale MC, Kessler RC, Heath AC, Eaves LJ (1992): Major depression and generalized anxiety disorder. Same genes, (partly) different environments? *Arch Gen Psychiatry* 49:716–722.
- Roy MA, Neale MC, Pedersen NL, Mathe AA, Kendler KS (1995): A twin study of generalized anxiety disorder and major depression. *Psychol Med* 25:1037–1049.
- Watson D (2005): Rethinking the mood and anxiety disorders: A quantitative hierarchical model for DSM-V. *J Abnorm Psychol* 114:522–536.
- Grant DM, Beck JG, Marques L, Palyo SA, Clapp JD (2008): The structure of distress following trauma: Posttraumatic stress disorder, major depressive disorder, and generalized anxiety disorder. *J Abnorm Psychol* 117:662–672.
- Moffitt TE, Harrington H, Caspi A, Kim-Cohen J, Goldberg D, Gregory AM, *et al.* (2007): Depression and generalized anxiety disorder: Cumulative and sequential comorbidity in a birth cohort followed prospectively to age 32 years. *Arch Gen Psychiatry* 64:651–660.
- Beesdo K, Pine DS, Lieb R, Wittchen HU (2010): Incidence and risk patterns of anxiety and depressive disorders and categorization of generalized anxiety disorder. *Arch Gen Psychiatry* 67:47–57.
- Aldao A, Mennin DS, Linardatos E, Fresco DM (2010): Differential patterns of physical symptoms and subjective processes in generalized anxiety disorder and unipolar depression. *J Anxiety Disord* 24: 250–259.
- Lawrence AE, Liverant GI, Rosellini AJ, Brown TA (2009): Generalized anxiety disorder within the course of major depressive disorder: Examining the utility of the DSM-IV hierarchy rule. *Depress Anxiety* 26: 909–916.
- Barlow DH (2000): Unraveling the mysteries of anxiety and its disorders from the perspective of emotion theory. *Am Psychol* 55:1247–1263.
- Clark LA, Watson D (1991): Tripartite model of anxiety and depression: Psychometric evidence and taxonomic implications. *J Abnorm Psychol* 100:316–336.
- Watson D, Clark LA, Weber K, Assenheimer JS, Strauss ME, McCormick RA (1995): Testing a tripartite model: II. Exploring the symptom structure of anxiety and depression in student, adult, and patient samples. *J Abnorm Psychol* 104:15–25.
- Watson D, Weber K, Assenheimer JS, Clark LA, Strauss ME, McCormick RA (1995): Testing a tripartite model: I. Evaluating the convergent and discriminant validity of anxiety and depression symptom scales. *J Abnorm Psychol* 104:3–14.
- Aldao A, Nolen-Hoeksema S (2012): When are adaptive strategies most predictive of psychopathology? *J Abnorm Psychol* 121:276–281.
- Ionescu DF, Niciu MJ, Mathews DC, Richards EM, Zarate CA Jr (2013): Neurobiology of anxious depression: A review. *Depress Anxiety* 30:374–385.
- Etkin A, Wager TD (2007): Functional neuroimaging of anxiety: A meta-analysis of emotional processing in PTSD, social anxiety disorder, and specific phobia. *Am J Psychiatry* 164:1476–1488.
- Etkin A, Schatzberg AF (2011): Common abnormalities and disorder-specific compensation during implicit regulation of emotional processing in generalized anxiety and major depressive disorders. *Am J Psychiatry* 168:968–978.

Neurobiological Signatures of Anxiety and Depression in Resting-State fMRI

20. Maier ME, di Pellegrino G (2012): Impaired conflict adaptation in an emotional task context following rostral anterior cingulate cortex lesions in humans. *J Cogn Neurosci* 24:2070–2079.
21. Beesdo K, Lau JY, Guyer AE, McClure-Tone EB, Monk CS, Nelson EE, *et al.* (2009): Common and distinct amygdala-function perturbations in depressed vs anxious adolescents. *Arch Gen Psychiatry* 66:275–285.
22. Fox MD, Snyder AZ, Vincent JL, Corbetta M, Van Essen DC, Raichle ME (2005): The human brain is intrinsically organized into dynamic, anticorrelated functional networks. *Proc Natl Acad Sci U S A* 102:9673–9678.
23. Etkin A, Prater K, Schatzberg A, Menon V, Greicius M (2009): Disrupted amygdalar subregion functional connectivity and evidence of a compensatory network in generalized anxiety disorder. *Arch Gen Psychiatry* 66:1361.
24. Roy AK, Fudge JL, Kelly C, Perry JS, Daniele T, Carlisi C, *et al.* (2013): Intrinsic functional connectivity of amygdala-based networks in adolescent generalized anxiety disorder. *J Am Acad Child Adolesc Psychiatry* 52:290–299.e292.
25. Greicius MD, Flores BH, Menon V, Glover GH, Solvason HB, Kenna H, *et al.* (2007): Resting-state functional connectivity in major depression: Abnormally increased contributions from subgenual cingulate cortex and thalamus. *Biol Psychiatry* 62:429–437.
26. Hamilton JP, Furman DJ, Chang C, Thomason ME, Dennis E, Gotlib IH (2011): Default-mode and task-positive network activity in major depressive disorder: Implications for adaptive and maladaptive rumination. *Biol Psychiatry* 70:327–333.
27. Hamilton JP, Chen G, Thomason ME, Schwartz ME, Gotlib IH (2011): Investigating neural primacy in major depressive disorder: Multivariate Granger causality analysis of resting-state fMRI time-series data. *Mol Psychiatry* 16:763–772.
28. Sheline YI, Price JL, Yan Z, Mintun MA (2010): Resting-state functional MRI in depression unmasks increased connectivity between networks via the dorsal nexus. *Proc Natl Acad Sci U S A* 107:11020–11025.
29. Anand A, Li Y, Wang Y, Wu J, Gao S, Bukhari L, *et al.* (2005): Activity and connectivity of brain mood regulating circuit in depression: A functional magnetic resonance study. *Biol Psychiatry* 57:1079–1088.
30. Veer IM, Beckmann CF, van Tol MJ, Ferrarini L, Milles J, Veltman DJ, *et al.* (2010): Whole brain resting-state analysis reveals decreased functional connectivity in major depression. *Front Syst Neurosci* 4:pii:41.
31. Horn DI, Yu C, Steiner J, Buchmann J, Kaufmann J, Osoba A, *et al.* (2010): Glutamatergic and resting-state functional connectivity correlates of severity in major depression—the role of pregenual anterior cingulate cortex and anterior insula. *Front Syst Neurosci* 4:pii:33.
32. Tao H, Guo S, Ge T, Kendrick KM, Xue Z, Liu Z, *et al.* (2013): Depression uncouples brain hate circuit. *Mol Psychiatry* 18:101–111.
33. Baur V, Hanggi J, Langer N, Jancke L (2013): Resting-state functional and structural connectivity within an insula-amygdala route specifically index state and trait anxiety. *Biol Psychiatry* 73:85–92.
34. Dennis EL, Gotlib IH, Thompson PM, Thomason ME (2011): Anxiety modulates insula recruitment in resting-state functional magnetic resonance imaging in youth and adults. *Brain Connect* 1:245–254.
35. Kim MJ, Gee DG, Loucks RA, Davis FC, Whalen PJ (2011): Anxiety dissociates dorsal and ventral medial prefrontal cortex functional connectivity with the amygdala at rest. *Cereb Cortex* 21:1667–1673.
36. Watson D, Clark LA (1991): *The Mood and Anxiety Symptom Questionnaire*. Iowa City, IA: University of Iowa.
37. Etkin A, Prater KE, Hoefl F, Menon V, Schatzberg AF (2010): Failure of anterior cingulate activation and connectivity with the amygdala during implicit regulation of emotional processing in generalized anxiety disorder. *Am J Psychiatry* 167:545–554.
38. American Psychiatric Association (1994): *Diagnostic and Statistical Manual of Mental Disorders*, 4th ed. Washington, DC: American Psychiatric Press.
39. Sheehan DV, Lecrubier Y, Sheehan KH, Amorim P, Janavs J, Weiller E, *et al.* (1998): The Mini-International Neuropsychiatric Interview (M.I.N.I.): The development and validation of a structured diagnostic psychiatric interview for DSM-IV and ICD-10. *J Clin Psychiatry* 59 (suppl 20):22–33; quiz 34–57.
40. Sheehan DV, Lecrubier Y, Harnett-Sheehan K, Janavs J, Weiller E, Keskiner A, *et al.* (1997): Reliability and validity of the MINI International Neuropsychiatric Interview (M.I.N.I.): According to the SCID-P. *European Psychiatry* 12:232–241.
41. Glover GH, Lai S (1998): Self-navigated spiral fMRI: Interleaved versus single-shot. *Magn Reson Med* 39:361–368.
42. Kim DH, Adalsteinsson E, Glover GH, Spielman DM (2002): Regularized higher-order in vivo shimming. *Magn Reson Med* 48:715–722.
43. Glover GH, Li TQ, Ress D (2000): Image-based method for retrospective correction of physiological motion effects in fMRI: RETRO-ICOR. *Magn Reson Med* 44:162–167.
44. Song XW, Dong ZY, Long XY, Li SF, Zuo XN, Zhu CZ, *et al.* (2011): REST: A toolkit for resting-state functional magnetic resonance imaging data processing. *PLoS One* 6:e25031.
45. Desikan RS, Segonne F, Fischl B, Quinn BT, Dickerson BC, Blacker D, *et al.* (2006): An automated labeling system for subdividing the human cerebral cortex on MRI scans into gyral based regions of interest. *Neuroimage* 31:968–980.
46. Eickhoff SB, Stephan KE, Mohlberg H, Grefkes C, Fink GR, Amunts K, *et al.* (2005): A new SPM toolbox for combining probabilistic cytoarchitectonic maps and functional imaging data. *Neuroimage* 25:1325–1335.
47. Patenaude B, Smith SM, Kennedy DN, Jenkinson M (2011): A Bayesian model of shape and appearance for subcortical brain segmentation. *Neuroimage* 56:907–922.
48. Liston C, Chen AC, Zebly BD, Drysdale AT, Gordon R, Leuchter B, *et al.* (2014): Default mode network mechanisms of transcranial magnetic stimulation in depression [published online ahead of print Feb 5]. *Biol Psychiatry*.
49. Chen AC, Oathes DJ, Chang C, Bradley T, Zhou ZW, Williams LM, *et al.* (2013): Causal interactions between fronto-parietal central executive and default-mode networks in humans. *Proc Natl Acad Sci U S A* 110:19944–19949.
50. Beck AT, Steer RA (1993): *Beck Anxiety Inventory Manual*. San Antonio, TX: Psychological Corporation.
51. Beck AT, Steer RA, Brown GK (1996): *Manual for Beck Depression Inventory II (BDI-II)*. San Antonio, TX: Psychological Corporation.
52. Meyer TJ, Miller ML, Metzger RL, Borkovec TD (1990): Development and validation of the Penn State Worry Questionnaire. *Behav Res Ther* 28:487–495.
53. Spielberger CD, Gorsuch RL, Lushene RE (1970): *Manual for the State-Trait Anxiety Inventory*. Palo Alto, CA: Consulting Psychologists Press.
54. Fox MD, Buckner RL, White MP, Greicius MD, Pascual-Leone A (2012): Efficacy of transcranial magnetic stimulation targets for depression is related to intrinsic functional connectivity with the subgenual cingulate. *Biol Psychiatry* 72:595–603.
55. Zuo XN, Di Martino A, Kelly C, Shehzad ZE, Gee DG, Klein DF, *et al.* (2010): The oscillating brain: Complex and reliable. *Neuroimage* 49:1432–1445.
56. Biswal BB, Mennes M, Zuo XN, Gohel S, Kelly C, Smith SM, *et al.* (2010): Toward discovery science of human brain function. *Proc Natl Acad Sci U S A* 107:4734–4739.
57. Gusnard DA, Raichle ME, Raichle ME (2001): Searching for a baseline: Functional imaging and the resting human brain. *Nat Rev Neurosci* 2:685–694.